Testing and Monitoring in Railway Tracks

Eduardo Fortunato and André Paixão

Abstract Railway tracks may be perceived as simple physical structures, but in fact they entail a significant level of complexity as refers to the assessment and prediction of their transient and long-term behaviors. These mostly result from the intrinsic characteristics of their components and of the dynamic interaction with the successive passing trains at different speeds and with different loading characteristics. The railway industry's traditionally conservative approach to new technologies and the limited access, mostly for safety reasons, to related infrastructures somewhat hinder new developments and make it difficult to obtain further insight into the behavior of these structures. To overcome these limitations, advanced methods have been proposed for characterizing the materials that integrate the tracks and a few developments have been implemented in the monitoring of the structures under static and dynamic loading conditions. The information obtained has been essential to validate track models and to predict the transient response and the degradation behavior of the structures and their materials. This has promoted the introduction of new materials and construction methods with a view to improve the structural and environmental performances of railway infrastructures. The work presented herein provides an overview of current and advanced characterization and monitoring techniques, which are exemplified by a few applications concerning both R&D and consulting initiatives.

Keywords Railway tracks · Testing · Instrumentation · Monitoring

E. Fortunato (✉) · A. Paixão
LNEC, National Laboratory for Civil Engineering, Lisbon, Portugal
e-mail: efortunato@lnec.pt

A. Paixão
e-mail: apaixao@lnec.pt

C. Chastre et al. (eds.), *Advances on Testing and Experimentation in Civil Engineering*, Springer Tracts in Civil Engineering,
https://doi.org/10.1007/978-3-031-05875-2_10

1 Introduction

The traditional railway track integrates both the superstructure (rails, sleepers, fastenings, and ballast) and the substructure that includes the sub-ballast and the subgrade; the upper part of the latter is usually called the capping layer or form layer (Fig. 1). The functioning of these elements is relatively complex, leading to a non-linear behavior of the structure when subjected to loading and unloading cycles caused by the passage of vehicles [1, 2].

The rails accommodate the wheel loads and distribute these loads across the sleepers. They also guide the wheels in a lateral direction. The rails may also act as electrical conductors for the signal circuit and as electrical conductors in an electrified line. In ballasted tracks, the rails are held by sleepers that attenuate and distribute the forces transmitted by the rolling stock to the ballast.

The sleepers also play an important role in the stability of the track, in its plane, because it is their own weight and the fact that they are embedded in the ballast that allows the track to withstand the lateral forces produced by the rolling stock and the forces associated with the thermal variation of long welded rails. Rail fastenings can be either rigid (typically for wooden sleepers) or flexible (for concrete sleepers) and are intended to ensure the correct positioning of the rails on the sleepers, by considering vertical, transverse, and longitudinal forces. The rail pads provide track resiliency, influencing its dynamic response, and reduce wear on sleepers.

The ballast layer is one of the most important elements of conventional tracks and plays an important role in the economic efficiency and sustainability of railway transport. The ballast layer—usually 20–40 cm thick—is composed of coarse hard rock particles of nearly uniform grain size distribution and its functions include the transmission and dissipation of the cyclic loads imposed by the passing trains (transmitted from the rails to the sleepers) to the underlying layers, by simultaneously ensuring the horizontal position of the track and providing proper drainage. Throughout its life cycle, the ballast layer densifies, mainly due to particle breakage and subgrade soil pumping, under successive impact loads, maintenance actions and climatic effects [3, 4]. Plastic deformations [5] and differential settlements in the supporting layers lead to changes in the position of the rails, to track defects and wear of components, thus reducing the performance of this infrastructure and eventually leading to the need to perform maintenance interventions to reestablish rail geometry.

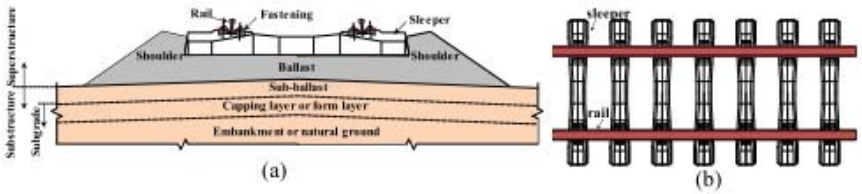

Fig. 1 Ballasted railway track: **a** schematic cross section; **b** schematic track plan view

The methods for characterizing materials and for modeling and monitoring the behavior of the railway track have evolved, allowing to design, build and maintain these structures in a more appropriate manner. In this chapter, we provide an overview of some current and advanced characterization and monitoring techniques.

2 Aspects of the Characterization of Materials

2.1 Advances in Ballast Particle Morphology

The natural aggregate for the ballast layer is one of the best controlled raw materials. Compressive particle-particle contact, particle-particle and particle-sleeper friction and imbrication are the major mechanical actions resulting from traffic and heavy maintenance interventions. Cubic shape, rough faces, and sharp edges favor imbrication, thus avoiding rolling or significant translational movements, resulting in higher layer stability and less contact forces between particles (by increasing contact points).

To ensure that the material undergoes limited degradation and preserves its optimal morphological parameters throughout its lifecycle, some mechanical and geometric properties are usually required for ballast particles, which are defined in specific regulations, by considering well-established characterization procedures [6, 7].

Though extensively validated, some of these procedures have limitations. Traditionally, particle morphology is evaluated using several classification criteria and a variety of indices or descriptors have been proposed by different authors, which were mostly presented over the last century [8]. The most practical and basic approach consists of sieving the material, but this makes only possible to capture partial particle size. Maximum and minimum particle dimensions can be determined manually using calipers, but this method is slow, subjective [9] and prone to human error [10]. Moreover, these approaches are reductive of the 3D aspects of the particles, and do not take advantage of recent knowledge and current automated methods and of image analysis approaches to fully characterize these aggregates. These new procedures allow, for example, to carry out a thorough analysis of the wear of the particles, when they are subjected to mechanical actions. Furthermore, computational advances in hardware and simulation methods led to the development of discrete element numerical models of railway tracks that demand a deep knowledge of particle shape. When properly calibrated, these models can be used to analyze the effects of traffic and mechanical maintenance actions on particle shape evolution, layer stability and track dynamic behavior [11].

Three-dimensional scanning of natural objects such as ballast particles can be performed with sub-millimeter precision, resulting in 3D models with up to a few millions of vertices and facets. Various methods are available for particle scanning and morphology analysis [8]. Some of them are expensive, such as those related to the use of X-ray computed tomography (CT) images [12]; others are either based on

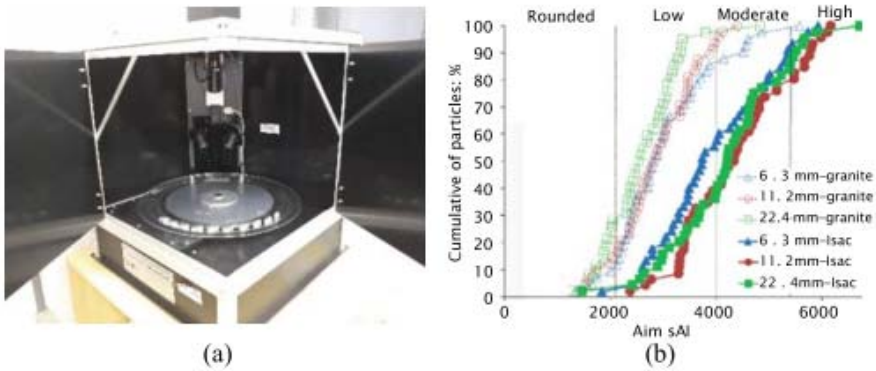

Fig. 2 Particle morphology: **a** AIMS equipment; **b** angularity [14]

2D particle morphology characterization or are only applicable to limited particle dimensions [13].

Delgado et al. [14] used the Aggregate Image Measurement System (AIMS) [15] (Fig. 2a) to quantify the sphericity, surface texture (roughness) and angularity of aggregate particles, based on the digital evaluation of a set of particles. They compared ballast particles with different nominal diameters (6.3, 11.2 and 22.4 mm) of inert steel aggregates for construction (ISAC) containing granite particles. The values obtained for particle sphericity and surface texture were similar in both materials. On the contrary, angularity was low in granite and was low/moderate to high in slag (Fig. 2b). This aspect can help explain the improved performance of slag particles when compared with that of granite aggregate, under the same loading conditions [16–18].

Several authors employed laser scanning to study ballast particle shape or to assemble particle libraries for Discrete Element Method simulations [19]. Jerónimo et al. [20] developed some studies with a portable laser scanner using a laser scanner that uses a laser emitter, 3 high definition cameras and 8 LEDs placed around the cameras (Fig. 3a). Image resolution was 0.05 mm and accuracy was at least 0.04 mm,

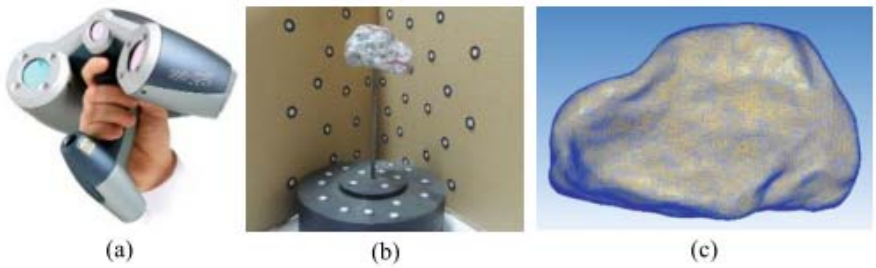

Fig. 3 Laser scanning procedure: **a** portable laser scanner; **b** support pedestal and screen with reflective targets; **c** triangle mesh of the particle at 1 mm resolution [20]

which made it suitable for small, complex-shaped ballast particles. The point cloud and the particle size were obtained with the aid of retroreflective targets placed on the object and/or the surrounding area (Fig. 3b). The targets were recognized by the scanner and a reference system was automatically generated. The cameras also detected ambient light reflected by the scanned surface and recorded color.

Based on digital models of a set of particles (Fig. 3c), it was possible to calculate geometric parameters and their evolution in face of particle degradation during mechanical testing (Fig. 4). Laser scanning detects and quantifies particle wear and fragmentation in a way that is not possible with traditional methods, which can only quantify volume/mass loss and qualitative shape change. In that study more sophisticated analyses were explored, such as calculation of sphericity.

Considering the capabilities of the photogrammetry and its recent advances, Paixão et al. [21] presented a cost-efficient photogrammetry method for 3D reconstruction of ballast particles (Fig. 5), as an alternative to the significantly expensive laser scanning. They compared these approaches with the laser scanning method employed in the previous study, using the same set of granite ballast particles, and considering their condition after fragmentation and wear tests. The authors compared the laser scan and photogrammetry meshes of 18 digital particles. They obtained

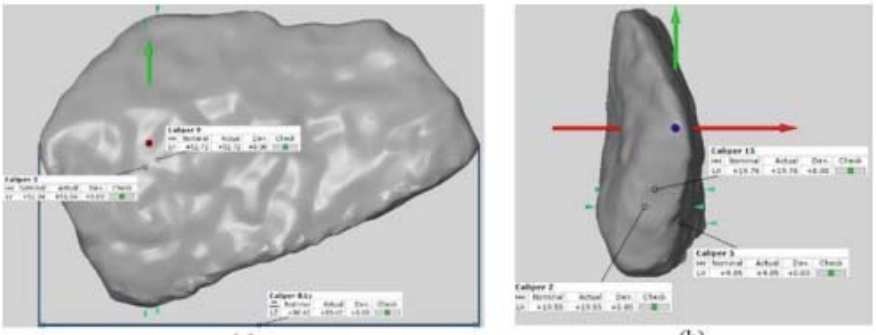

Fig. 4 Digital determination of particle dimensions: **a** L (maximum); **b** S (smallest)

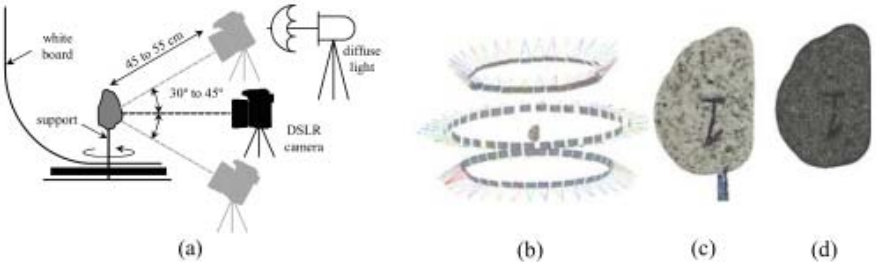

Fig. 5 Workflow: **a** setup of the photography session; **b** camera pose calculation, image matching and sparse reconstruction; **c** dense reconstruction; **d** generated mesh [21]

digital models of equivalent or higher quality with photogrammetry, namely: (i) peak differences were below 1 mm; (ii) more than 50% of the surface area showed differences less than 0.1 mm; (iii) average standard deviation of the deviations was about 0.1 mm.

According to the results, the authors considered the performance of the photogrammetry as very good, allowing for advanced and automated particle geometry analyses: sub-millimeter accuracy can be achieved using cheaper equipment and software.

Other recent applications of close-range photogrammetry have evidenced the potential of this approach for low cost detailed 3D scanning of coarse aggregates [22].

Paixão and Fortunato [23] used this method to compare the abrasion evolution of a steel slag with a granite aggregate that fulfilled the requirements for ballast in Europe. An analysis was performed on the evolution of the morphology of aggregates, which included both conventional and advanced approaches, as well as a spherical harmonic analysis of a 3D digitalization of the particles obtained by close-range photogrammetry.

Quantitative analyses were conducted on the abrasion and 3D morphology evolution of particles by micro-Deval testing. It should be noted that due to the phasing implemented in the micro-Deval test (0, 2000 and 14,000 revolutions), a total of 180 digital models (30 particles from each aggregate, in 3 phases of the micro-Deval test) were constructed (averaging around 290,000 vertices and 580,000 faces), using a total of nearly 20 thousand captured images. To elucidate on the detail of the scans achieved with this method, on average, the density of the meshes was about 38 vertices/mm^2. Due to the large number of manual measurements that would have to be performed on the 60 particles, for each of the three phases of the test, and to avoid the typical errors introduced in these types of measurements, an automated digital measuring tool was developed in MATLAB environment. Among other parameters, this tool makes it possible to determine the maximum, L, intermediate, I, and smallest, S, dimensions, volume, V, surface area, A, sphericity, ψ, and the flattening ratio, $p = S/I$, elongation ratio, $q = I/L$, degree of equancy, S/L, and Form index, $F = p/q$. Figure 6 presents an example of the automated analysis of a steel slag particle using this tool.

This study demonstrated quantitatively that the slag particles were richer than the granite ones, in terms of angularity and surface texture, in all analyzed stages of the micro-Deval test. This was evidenced and quantified by the morphology indices that were calculated by both the spherical harmonic analysis and the 3D mesh analysis of the particle's surfaces, as refers to surface curvature or asperity radius (Fig. 7). The initial morphology of the slag particles was more complex and irregular, and they retained these characteristics for longer than the granite during the abrasion test.

Moreover, slag particles underwent similar or less surface wear, although they had more asperities, being hence more prone to abrasion, breaking and chipping of protruding edges and vertices. In particular, the 3D mesh analysis showed consistently less surface wear in the slag aggregate than in the granite one, for different

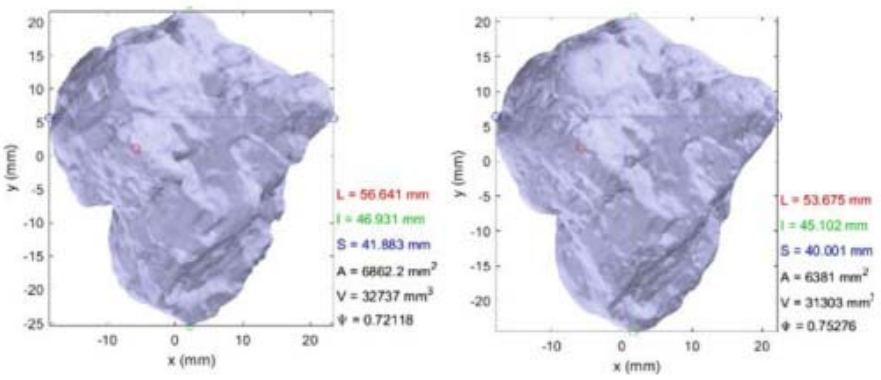

Fig. 6 Abrasion of a steel slag particle: initial (left) and final configuration (right) [23]

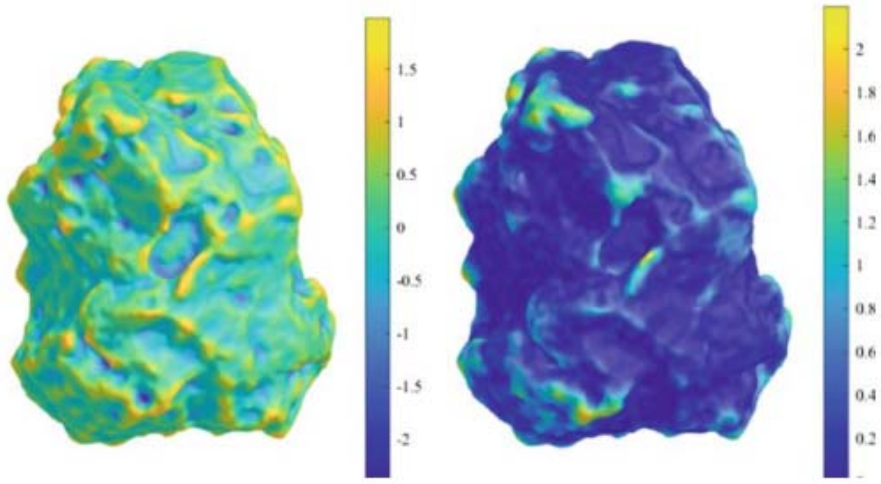

Fig. 7 Example of curvature [1/mm] (left) and wear [mm] (right) on a slag particle [23]

ranges of surface curvatures. The granite ballast showed lower micro-Deval abrasion coefficients than the slag aggregate in both the dry and the wet procedures, which could imply that the granite had greater resistance to abrasion. However, the advanced morphological analyses showed that the particles of the two materials underwent similar abrasion, in terms of both mass and volume loss. This suggests that the micro-Deval abrasion test does not fully translate the abrasion mechanism of these aggregates and may be especially disadvantageous for the slag aggregate. Regarding the traditional morphologic characterization, the results were very similar for both materials, which suggests that traditional characterization methods may not be adequate for this type of in-depth analyses. Nevertheless, the characterization of the steel slag particles in a modified Zingg diagram [9] was more uniform and their

evolution path was also shorter, meaning that the slag particles morphologic changes were smaller, which agrees with the results obtained with the more advanced methods. Since the results of this work indicate that slag particles provide better interlocking and show less or comparable surface wear, thus, in terms of particle morphology and resistance to abrasion, slag appears to be equally or better suited to the application in railway ballast layers. Considering that the shear strength and stability of the ballast layer increase with the angularity of its particles, these findings contribute to demonstrate that steel slag can be a source of aggregate for railway ballast and may even achieve a higher level of mechanical and environmental performances, as previously mentioned.

In conclusion, the tasks that can benefit from this kind of methods are as follows: rigorous and replicable measurement of volume, surface area and roughness; quantitative assessment of wear and fragmentation; production of digital particle libraries, which can be shared globally or used to create digital particles for discrete element simulations that are on the way to becoming a useful method for more accurate ballast simulation.

2.2 Ballast Mechanical Behavior Under Cyclic Loading

In general terms, there are two ways to analyze ballast behavior: by a micromechanical approach, based on the physical and mechanical characteristics of the particles; and by a macromechanical approach that considers the behavior of the granular medium. In the latter case, compacted samples are characterized [17, 24, 25], or physical models are tested, in real or reduced scale, considering either some parts or the totality of the structure. Compared to in situ characterization methods, laboratory physical modelling has several advantages regarding repeatability and reproduction of different settings. However, some aspects that characterize the complex behavior of the track (e.g., the density of the ballast layer), are hardly adequately reproduced in laboratory, which may affect the validity of the results.

On a physical model recently built at National Laboratory for Civil Engineering in Portugal it was possible to perform a few tests to evaluate accumulated settlements over a relatively large number of load cycles of the ballast layer [5]. The tests comprised cyclic loading on one concrete monoblock sleeper embedded in ballast, with a conventional and modern track foundation, and an Iberian track gauge. A schematic view of the test and photos are shown in Fig. 8. Confining metallic walls were devised to minimize friction between the soils/aggregates and the walls. The subgrade and sub-ballast layers were heavily compacted during the construction phase using a compaction roller. The sub-ballast was compacted in sublayers of 0.05 m. The ballast layer was compacted with both the compaction roller and the mobile Cobra TTe hammer.

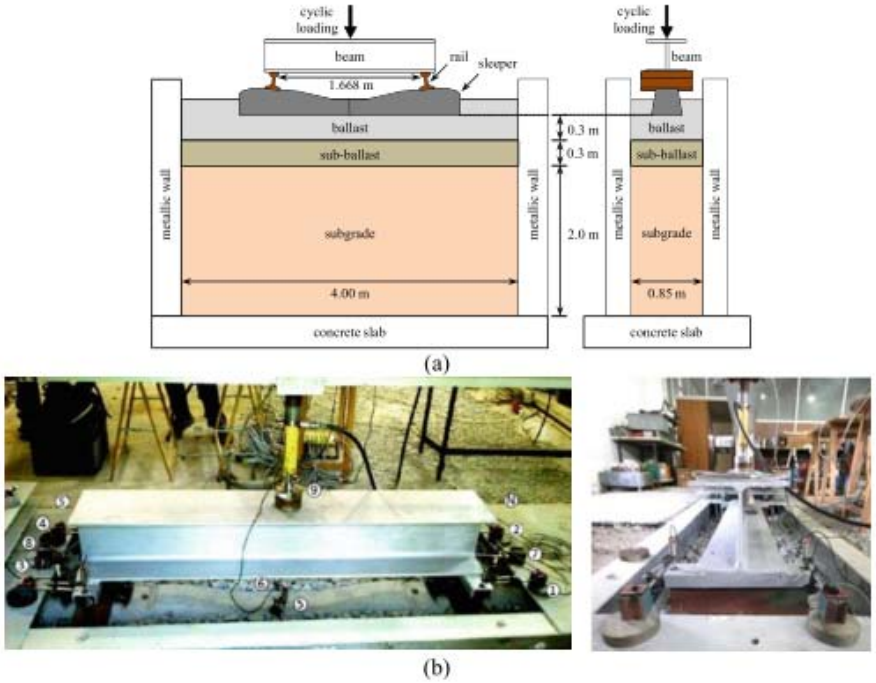

Fig. 8 Physical model: **a** scheme (front and lateral views); **b** test (front and lateral views) [5]

The loading was transmitted from one hydraulic actuator to the sleeper by a spreader steel beam. The displacements were measured with LVDTs placed at positions 1–9, as shown in Fig. 8: positions 1–4 on the rails; positions 5–8 on the sleeper and position 9 is the base of the actuator.

The simulated train loading was applied 5.5×10^5 times at a frequency of 1 Hz. The maximum load applied by the actuator was 100 kN, and the minimum load was 4 kN to avoid impacts on the sleeper. Assuming a typical maximum wheelset to sleeper load transmission of 50%, the load of 100 kN corresponded to an axle load of approximately 19.6 tones. Following an initial phase of rapid settlement measured on the sleeper (average of the four measured positions), the permanent deformation rate decreased nearly to zero, a phenomenon referred to as shakedown [26]. The representation in a logarithmic scale, in Fig. 9, shows however that for $N > 10^5$ the settlements continue progressing at an approximate log-linear rate. A small bump can be observed on the settlements curve before cycle 1×10^5, which was caused by a short interruption in the test to replace the actuator.

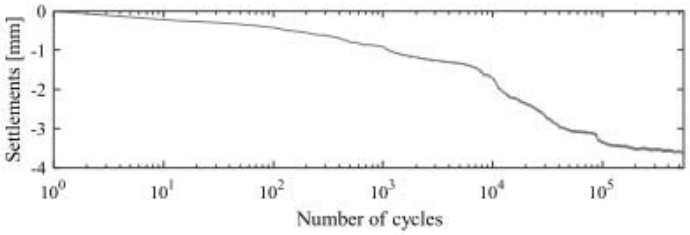

Fig. 9 Settlements measured on the sleeper [5]

3 Railway Track Characterization and Monitoring

3.1 Surface Wave Method in Testing the Railway Platform

The Surface Wave Method (SWM), which is based on the propagation of elastic surface waves along the ground, is a powerful method to assess the stiffness of the medium in depth [27]. As a geophysical method, it relies on the propagation of seismic waves across the medium with very low strain values, typically below 10^{-5}, making it possible to use the Linear Elasticity Theory to interpret the results. It allows fast and non-invasive testing, avoiding delays in the construction works and decreasing repairing costs in the tested locations; the equipment is compact, lightweight, and user-friendly.

This method was adopted in a research performed during the renewal of a Portuguese railway line platform (Northern Line), in which minimum values of the deformation modulus at the top of capping and sub-ballast layers were specified [28]. In that work, two techniques were used, i.e. the Spectral Analysis of Surface Waves (SASW) and the Continuous Surface Waves (CSW) [29]. From among the equipment used, reference is made to the following: an electro-mechanical vibrator with a controlling unit (for the CSW method, capable of generating loads up to 500 N); six 2 Hz geophones; a control unit for definition of parameters, for acquisition and analysis of load and geophones signals, as well as for data processing and data recording; hammers of different masses (for the SASW method); and a power generator. From the spectral records, the phase of the signal generated by the source in each geophone position was determined and the phase difference between the signals in each geophone and the coherence between signals was calculated. In the case of CSW, the minimum square method was used to determine the phase angle for each vibration frequency. Both the analysis and the processing of data regarding the SASW, as well as the inversion in the dispersion curve and the calculation of the variation of the shear modulus in depth, were performed with the software WINSASW 2.0 [30].

Figure 10a, b show some aspects of the tests performed on both the old and the renewed railway platforms. Figure 10c presents the profiles of the deformation modulus obtained in one place with the SASW, E_{SASW}, during the phases of renewal

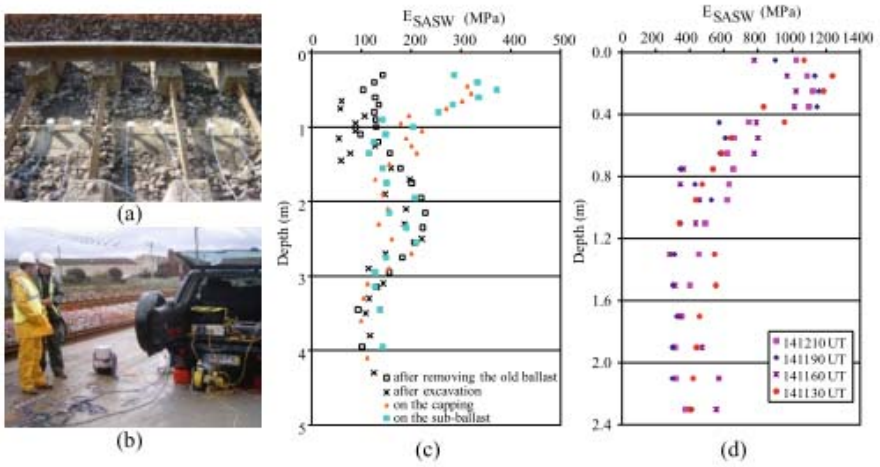

Fig. 10 Aspects of the tests: **a** SASW on the old track; **b** CSW on the renewed platform; **c** E_{SASW} in one place during the renewal; **d** E_{SASW} in some places in a newly built zone [28]

of the railway platform. The depth presented refers to the bottom of sleepers, prior to old ballast removal. The following comments can be made: the variation in the E_{SASW} is important, both in depth and between tests; following the old ballast removal, E_{SASW} values of about 140 MPa were measured from the surface, which are likely to correspond to a zone of higher compactness, due to rail traffic over the years; below and up to about 1.0–1.2 m depth, the average values of E_{SASW} ranged from 100 to 130 MPa; between that depth and around 2 m, E_{SASW} ranged between 200 and 230 MPa, reaching 100 MPa between this depth and above 3.5 m; the results obtained after excavation of a 0.35 m thickness seem to indicate that the consequent vertical stress reduction caused a decrease in the E_{SASW}, when compared with the values at the same depth before excavation, particularly up to about 1.5 m depth; after placing the 0.20 m thick capping layer of crushed limestone of well graded particle-size distribution, E_{SASW} increased to about 300 MPa in that layer; E_{SASW} in the sub-ballast layer (0.15 m) was about 300–350 MPa; the placement of that layer on the capping have increased the E_{SASW} of the latter to nearly 400 MPa.

Figure 10d shows the E_{SASW} obtained in a stretch where the railway platform was built on a new embankment. The tests were performed on the sub-ballast when the average water content was 1.4%, measured at a depth of 0.15 m, in the capping layer. We can draw the following conclusions: at the surface, corresponding to the sub-ballast and capping layers, E_{SASW} ranged from 800 to 1200 MPa; at the upper part of the embankment, down to about 0.30 m below the aggregate layers, E_{SASW} was 600–800 MPa; in the deeper layers, the values ranged from approximately 300–500 MPa.

In view of these results, it can be concluded that the SWM methods allow to estimate the deformability of the layers of the railway track substructure.

3.2 *Evaluating Track Stiffness with a Light Weight Deflectometer*

The falling weight deflectometer (FWD) is a non-destructive test that is traditionally used to perform stiffness assessment of road pavements. However, there are some reports of its use on railway tracks during substructure construction and on track under operation [31–33]. Paixão et al. [34] used the light falling weight deflectometer (LWD), a portable version of FWD, on sleepers to assess sleeper support conditions. These tests were carried out as part of a study that aimed to assess the influence of Under Sleeper Pads (USP) [35] on the behavior of transition zones between earthworks and civil engineering structures. Tests were performed on two similar underpasses in reinforced concrete closed frames (UP1 and UP2), located at a new single track of the Portuguese railway network. At UP1, 44 sleepers with USP were installed, while UP2 consisted of a standard track. The design established the construction of transition zones in accordance with demanding design requirements, similar to those implemented in new European high-speed railway lines [36] to avoid poor track performance [37]. Relevant aspects of the transition zones at UP1 and UP2 are presented in Fig. 11. The layers of the backfills were constructed with cement bound mixture (CBM) and unbound granular material (UGM).

The LWD applied a load impulse of 15 kN on a 0.10 m diameter plate at the center of each sleeper (Fig. 12a). A good coherence of results was observed between tests performed on sleepers with similar support conditions. Figure 12b presents the average deflection (δ_s) measured at the center of the sleepers, along two transition zones to UP1 and UP2. It can be observed that the δ_s of the sleepers without USP is about 50–100 mm. At UP1, the use of USP has increased δ_s up to about 450 mm.

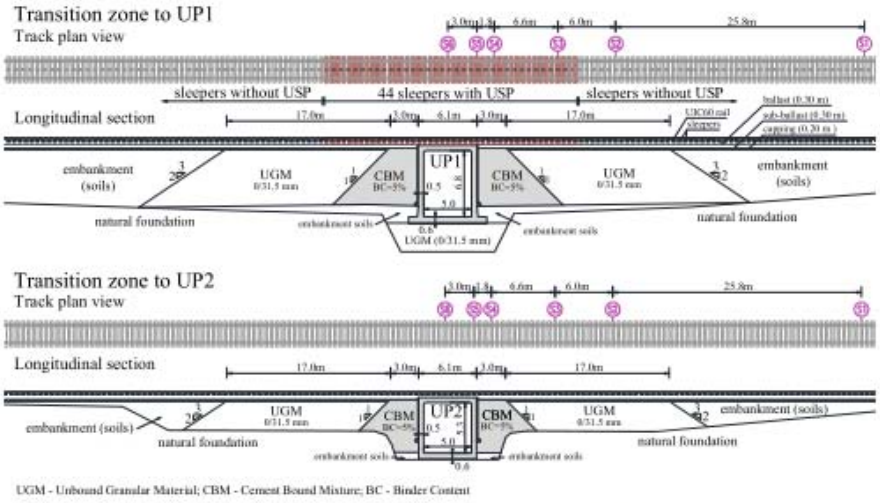

Fig. 11 Longitudinal profile of transition zones to UP1 and UP2 [34]

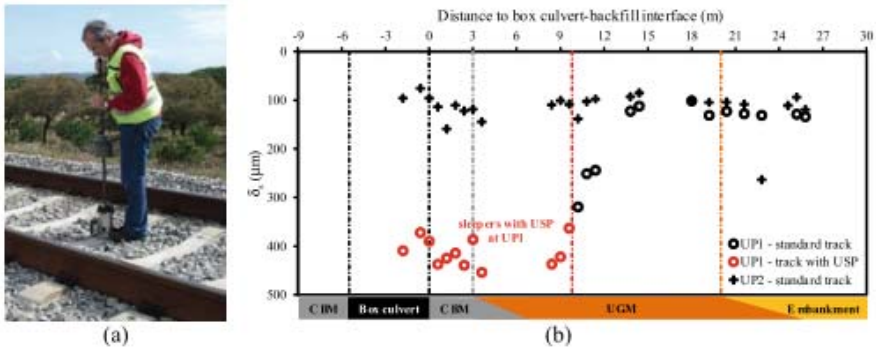

(a) (b)

Fig. 12 Sleeper deflections obtained in LWD tests: **a** test; **b** deflection [34]

Thus, it was found that the deflections of sleepers with USP were about 4–4.5 times higher than those obtained in sleepers without USP. At the transition between sleepers with and without USP, a variation in deflections is observed, denoting a transition in stiffness.

This unconventional procedure of using the LWD test at the center of the sleeper was found to be a very simple, straightforward, and effective procedure to swiftly assess track support conditions. Results indicate that an experienced operator can obtain good testing repeatability for several drops on the same sleeper.

3.3 Receptance Tests on the Track

Receptance tests are a very practical way to assess the dynamic behavior of the track [38]. The receptance tests that have been carried out by the authors consist of the excitation of the rail using an instrumented hammer, with input frequencies of up to 450 Hz, and of the evaluation of the track response using accelerometers installed on the rail web and sleepers. Figure 13 presents an example of a sampled time recording of the measured load impulse, along with its frequency content and respective rail response.

In order to characterize the dynamic behavior of the track across both transition zones described in 3.2, receptance tests were performed on specific sections identified in Fig. 11: S1 on open track; S2 and S3 on the UGM; S4 on the CBM; S5 on the vertical alignment of the box culvert walls; and S6 at mid-span of the box culvert.

Figure 14 depicts the average receptance functions obtained in each section for frequencies between 25 and 450 Hz, corresponding to the range of impulse-acceleration signal coherence above 0.95. In general, apart from the results obtained in sections with USP, no significant differences can be observed between other receptance function curves along the transition zones. Regarding all sections, it is possible to identify a resonant frequency between 300 and 375 Hz, which corresponds to the

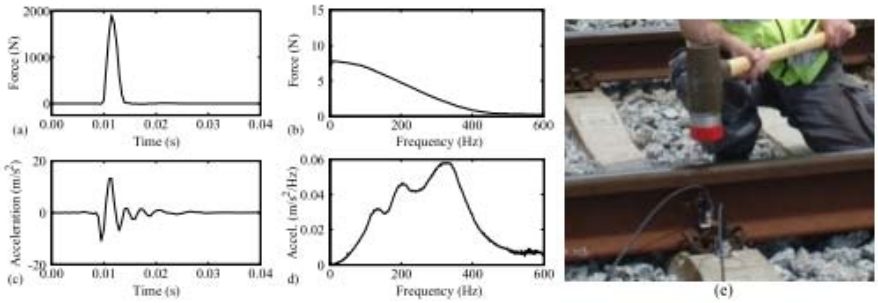

Fig. 13 Receptance test: **a** impulse time history; **b** frequency content; **c, d** respective rail responses in time and frequency domains; **e** test [34]

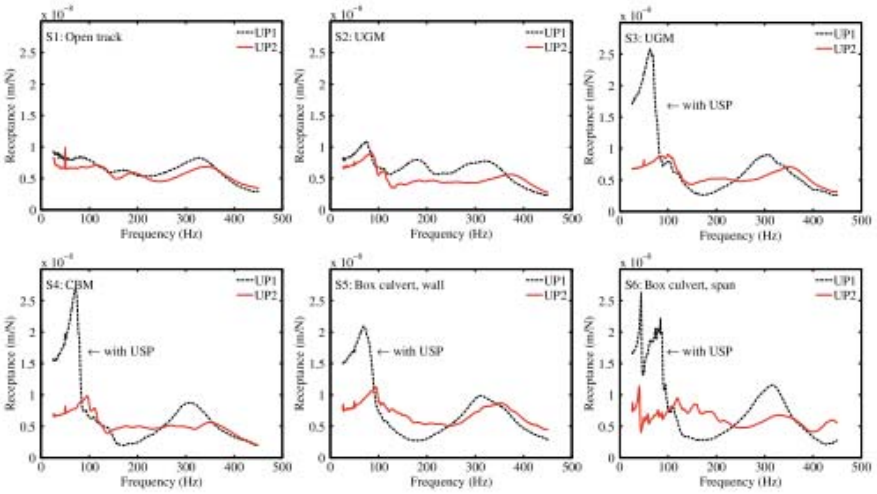

Fig. 14 Receptance functions obtained in each section [34]

vibration of the rail on the rail pads. The variability in the resonant frequency of the rail may be due to the uneven preload of the fastening system along the track, which generally influences the stiffness of rail pads [39]. The presence of USP at UP1 leads to a shift in the resonant frequency peak: the frequency of about 325 Hz in S1 and S2 (without USP) is reduced to about 308 Hz in S3 to S6 (with USP). This reduction is followed by a slight increase in the amplitude of the receptance function peak. The full track resonant frequency peaks are also visible at frequencies around 70 Hz for the track with USP (S3 to S6 in UP1) and at about 90–110 Hz without USP (the remaining sections). Higher amplitudes of the full track resonant frequency peaks are identified in sections with USP, indicating an increase in the dynamic flexibility of the track provided by these elements. It is worth noting the increased amplitude of the receptance function in lower frequencies ($f < 55$ Hz) in the presence of USP,

which denotes an increment of about 90% in the vertical flexibility of the track. The receptance curves in S3 (on the UGM) and S4 (on the CBM) are quite similar, within each transition zone. In S6, additional peaks were identified at 44 and 40 Hz, corresponding to the resonant frequencies of UP1 and UP2 box culverts.

The USP led to a reduction of about 18% in the full track resonant frequency and to an increase of about 50% in its receptance value. The rail resonant frequency peak was reduced by 5% and an increase of about 14% in the receptance value was observed.

Considering the previous results, we can conclude that the receptance tests on the rail, performed at different positions along the transition zones, allowed assessing the dynamic flexibility of the track for different support conditions. In addition, these tests can contribute to the calibration of numerical models of the railway track [40].

3.4 Evaluating Track Stiffness with the Portancemètre

Portancemètre is a non-destructive loading equipment that was initially developed to be used in earthworks [41]. It consists of a rolling vibrating wheel that makes it possible to perform continuous stiffness measurements and to obtain the respective values of the deformation modulus (E_{V2}) [42]. For some years now, Portancemètre has been used to assess the deformability of embankment layers and railway track platforms [36, 43].

The Portancemètre has had some modifications so as to be used to assess track stiffness, measured continuously on the rail [44]. The static load of the equipment may vary between 70 and 120 kN and the maximum dynamic load amplitude may increase up to 70 kN. The stiffness can be measured by exciting the track with a frequency of up to 35 Hz. The method has good repeatability and good correlation with other methods.

Figure 15 shows an on-site measurement and track stiffness at different excitation frequencies and a running speed of 6 km/h. There are relevant differences between

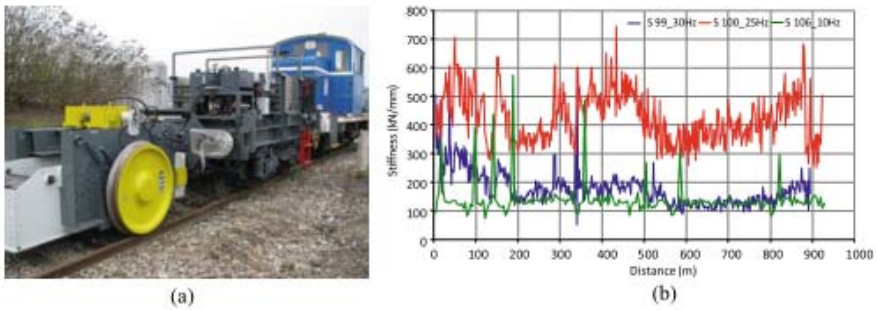

(a) (b)

Fig. 15 Portancemètre: **a** on-site measurement; **b** track stiffness values [44]

the results obtained with 25 Hz and other excitation frequencies, which may be explained by the closeness to the resonance frequency of the track. The results of 10 and 30 Hz excitations (probably lower and higher than the resonance frequency) are close to each other especially for low stiffness values.

Other methods have been developed for similar purposes. In any case, none of these methods are widely used [45].

3.5 *Evaluating Track Support Conditions with the Ground Penetrating Radar*

By detecting variations in the electromagnetic properties of the medium, the Ground Penetrating Radar (GPR) nondestructive technique can provide valuable and almost continuous information on the track condition. Examples of its application include detecting different materials in depth and identifying the degradation of the physical and mechanical characteristics of the track, such as ballast pockets, fouled ballast, poor drainage, subgrade settlement and transition problems [3, 46, 47].

In the last few years, the development of new GPR systems with higher antenna frequencies, better data acquisition systems, more user-friendly software, and new algorithms for calculation of materials properties have been leading to a more generalized use of GPR. As an example, Fig. 16 shows some results of the application of GPR on a railway track under renewal. The transition between the old and the renewed zones is clearly defined. As expected, the old section is more scattered and the interface between ballast and subgrade is not clear in some parts of the image, due to ballast fouling, whereas on the renewed section, a clearer identification is achieved and the two interfaces, between ballast and sub-ballast and sub-ballast and subgrade, are well revealed.

In other cases, it was possible to relate defects in track geometry with the information obtained with the GPR and to propose different rehabilitation techniques [48].

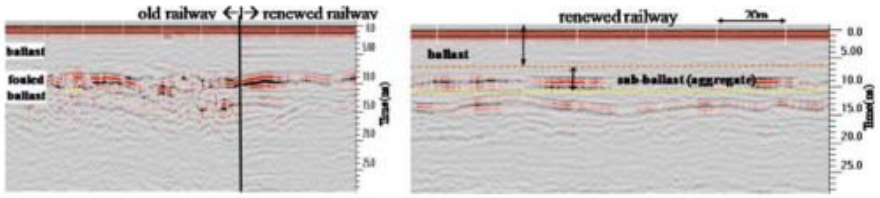

Fig. 16 GPR measurements on a transition between an old and a renewed track section (left) and on a renewed track section (right) [50]

With a view to improve GPR data analyses by an appropriate interpretation, it is necessary to obtain reliable information on the dielectric properties of tested materials. These characteristics affect GPR signal propagation, reflection, and data resolution; therefore, it is important to study which factors influence the dielectric constants and in which degree. De Chiara et al. [49] performed laboratory tests to determine the dielectric properties of infrastructure materials (clean granite ballast; silt soils; fouled ballast, as a mixture of the first two) under different conditions, in terms of both water content and fouling level, with GPR antennas of 5 different frequencies (400, 500, 900, 1000 and 1800 MHz). Fouling condition and the water content significantly influenced the dielectric values of the materials (Figs. 17 and 18). It is also known that ballast of different types of rock has different dielectric constant values [50].

Recent works using data from GPR surveys of railway infrastructures also explore the possibility of analyzing the GPR signal in the frequency domain to obtain further information about the track condition. Fontul et al. [51] presented an approach to analyze the data in both time and frequency domains, with a view to identify changes along significant lengths of railway lines that can correspond to either known track singularities or track pathologies.

The processing focuses on specific time intervals and frequency ranges of the signal that are more representative for identifying changes in the infrastructure. A

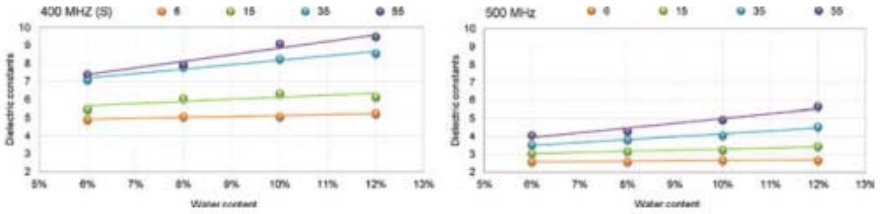

Fig. 17 Variation in the dielectric constant values of ballast with the fouling index (6–55), for the 400 MHz IDS suspended antenna (left) and the 500 MHz GSSI antenna (right) [49]

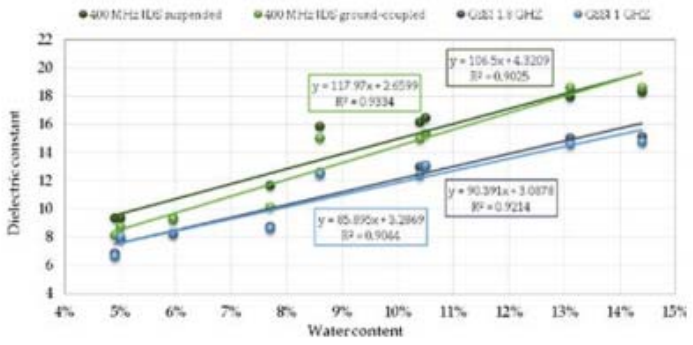

Fig. 18 Variation in the dielectric constant values of the soil with the water content [52]

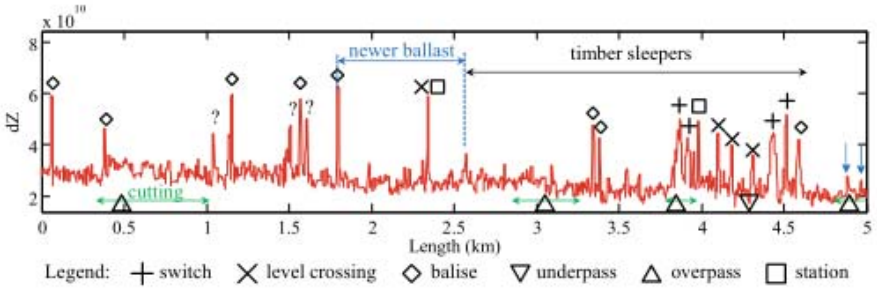

Fig. 19 Frequency domain analysis of GPR signal and correspondence with track events [51]

tool was developed to process, compare, and visualize the GPR data that can be further integrated with track geometry data and aerial photography for a user-friendly interpretation. Figure 19 depicts an example of this approach using the GPR data obtained in a 5-km section with an inspection vehicle equipped with 400 MHz GPR antennas by IDS. The figure shows the difference in signal amplitudes, dZ, in a specific frequency interval (0.7 and 2.0 GHz), calculated using a short sliding window (10 m), against the signal amplitude calculated using a wider sliding window (200 m). The results show a clear correspondence with specific track events.

3.6 Monitoring Dynamic Track Behavior Under Railway Traffic

Assessing the dynamic response of the railway track under passing trains is essential to understand its structural behavior and the evolution in its performance.

Within the scope of some research projects, the authors have used monitoring systems, including several devices, to measure variables related with the behavior of the track [53, 54]. These systems included various types of transducers to measure: (i) wheel loads; (ii) vertical displacements of the rail; (iii) rail-sleeper relative displacements (which are related to the deformation of the rail pad); (iv) vertical accelerations of the sleepers; (v) rail seat loads on the rail pads [55].

To estimate dynamic wheel loads and the reaction force at the rail seat portion of the sleeper, shear deformations on the rail can be measured between two sleepers (Fig. 20a). To compensate for any transversal eccentricity in the load applied by the train, at each measurement section of the rail, a pair of strain gauges was welded to each side of the web and connected to a full Wheatstone bridge. Each pair of strain gauges consisted of a shear rosette installed at the level of the neutral axis of the rail and with the respective sensitive patterns oriented $+45°$ and $-45°$ with respect to the rail longitudinal axis. At the longitudinal surface passing through the neutral axis of the rail, a pure shear state is developed, and the above orientations correspond to principal directions. Thus, deformations along these directions are equal in magnitude

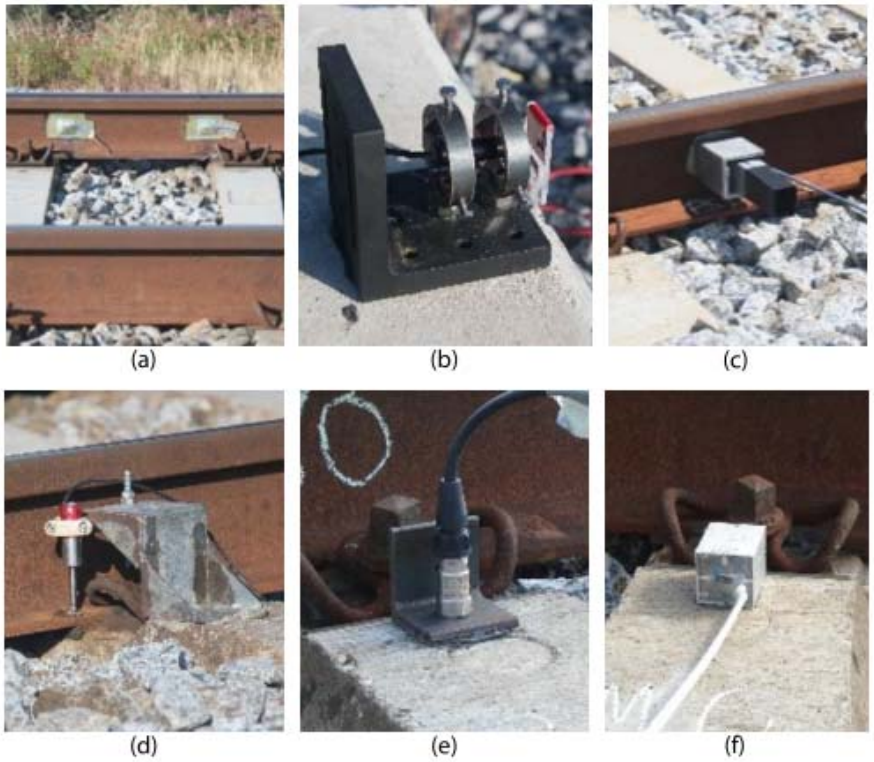

Fig. 20 Example of measuring systems: **a** strain gauges; **b** LASER diode; **c** PSD; **d** LVDT; **e** piezoelectric accelerometer; **f** MEMS accelerometers [54]

and opposite in sign ($\varepsilon_1 = -\varepsilon_2 = \varepsilon$) and shear strain is $\gamma = 2\varepsilon$. Absolute rail vertical displacements can be measured by optical systems based on a diode LASER module, mounted away from the track (Fig. 20b), and by a Position Sensitive Detector (PSD) module attached to a support fixed to the rail web (Fig. 20c). Using PSD transducers, it is possible to calculate rail displacements as trains pass by, measuring variations in the position of the LASER beam in the PSD. The vertical deformation of the rail pad can be assessed by a LVDT transducer placed between the rail and the sleeper (Fig. 20d). Vertical accelerations may be measured by piezoelectric accelerometers (Fig. 20e) and Micro Electro-Mechanical System accelerometers (MEMS) placed at the sleeper ends (Fig. 20f). In some studies, rail seat loads on the rail pads, using fiber optic sensors, are also measured. Typical and portable acquisition systems comprise a laptop computer, one or more acquisition units, as well as support units for the different types of transducers (Fig. 21).

There are many other devices and systems for instrumenting sleepers, the ballast layer and the railway substructure [56–59]. The data obtained with all these systems have led to deepen the knowledge about the behavior of the track and have enabled the calibration of numerical models.

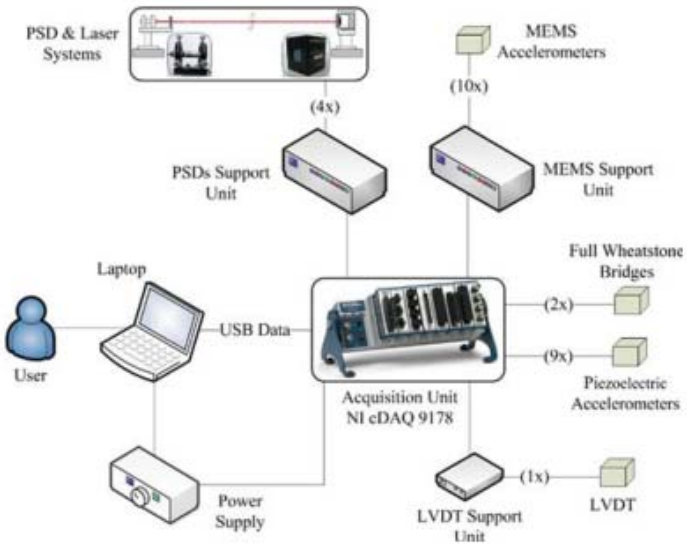

Fig. 21 Schematic representation of the data acquisition system [55]

4 On Board Monitoring with In-Service Railway Vehicles

Railway infrastructure managers run dedicated inspection vehicles to monitor the geometric quality of the track (among other aspects), to detect irregularities and to ensure safe running conditions of railway lines, in accordance with specific regulations [60]. The reconstruction of track geometry from track inspection cars is a well-established procedure and these vehicles are currently manufactured on an industrial basis by a few suppliers [61]. Modern inspection cars integrate an inertial measurement that uses the known measuring technique, by which the spatial position of a measuring sensor is determined by double integration of acceleration measurements [62]. Unfortunately, these inspections disturb the normal traffic operation, especially in networks with intensive traffic; are expensive and generally are carried out only a few times per year; and, consequently, do not provide a prompt identification of critical situations. Therefore, there is a need to develop alternative and expeditious methods to provide timely information on the performance and condition of the track, as implemented in recent years [63].

4.1 Non-dedicated Equipment

Due to the increasing sensing capabilities and cost reduction of sensors for smartphones, significant developments have been achieved as regards the application of micro-electro-mechanical systems (MEMS) to monitor transport systems. Paixão

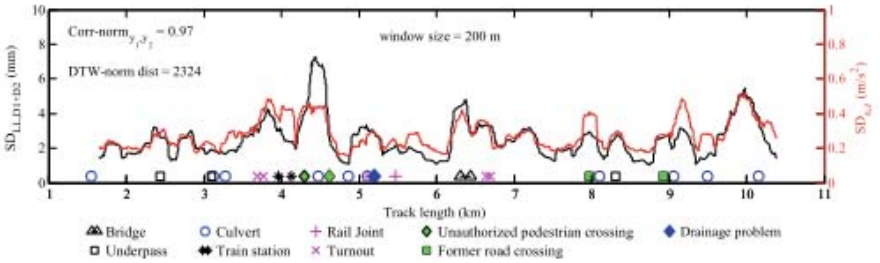

Fig. 22 $SD_{LL,D1+D2}$ and $SD_{a,z}$, considering a sliding-window size of 200 m [64]

et al. [64] presented an approach to use these technologies to perform continuous acceleration measurements on-board a passenger train with a smartphone. These measurements were analyzed and compared against the longitudinal level of the track geometry records and its degradation with time. That study also demonstrates further applicability of the approach to evaluate the structural performance of railway tracks, by assessing how different wavelengths and amplitudes of the geometric irregularities affect degradation, running safety, and ride comfort [65].

To demonstrate that the vertical accelerations measured inside the coach car are correlated to the longitudinal level of the track, Fig. 22 presents the standard deviation of the longitudinal level, $SD_{LL,D1+D2}$, regarding wavelength ranges $D1(3 < \lambda \leq 25m) + D2(25 < \lambda \leq 70m)$, and the standard deviation of the vertical accelerations, $SD_{a,z}$, considering a sliding-window size of 200 m. The normalized cross-correlation ($Corr - norm_{y1,y2}$) and dynamic time warping distance (DTW-norm dist) values [66, 67] between $SD_{LL,D1+D2}$ and $SD_{a,z}$ are also indicated. The very good correlation between the variables is visible on an 11-km railway stretch.

In order to justify the peak values of $SD_{LL,D1+D2}$ and $SD_{a,z}$, the authors analyzed the characteristics of the track, looking for any relevant structural aspects or sudden changes in the track structure (track discontinuity or singularities). About 30 relevant discontinuities were identified, including transition zones, rail joints, turnouts, bridges, underpasses, culverts, and stations, among others. Figure 23 presents some examples of these discontinuities, and their location was also included in Fig. 22. It can be observed that, in general, these correspond to the location of peak values

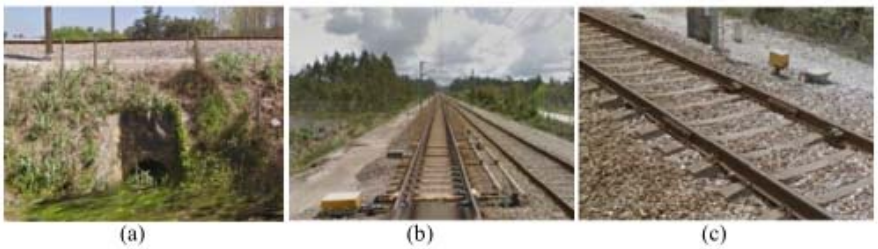

Fig. 23 Discontinuities: **a** culvert; **b** turnout; **c** rail joint [64] (Imagery ©2016 Google)

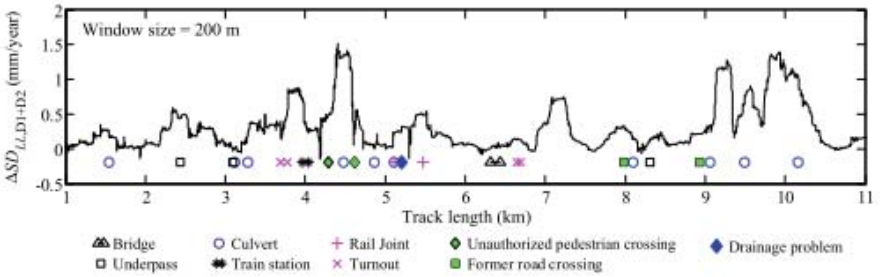

Fig. 24 $\Delta SD_{LL,D1+D2}$ considering a sliding window of 200 m [64]

of $SD_{LL,D1+D2}$ and $SD_{a,z}$. This suggests that these locations experience a higher geometric degradation and affect passenger comfort, which is in agreement with other studies [68–70].

Subsequently, to assess the actual track degradation rates, the authors analyzed the evolution of the $SD_{LL,D1+D2}$ between the surveys of 2013 and 2016, $\Delta SD_{LL,D1+D2}$. Figure 24 shows that most of the locations denoting higher degradation rates (higher $\Delta SD_{LL,D1+D2}$) generally also correspond to the locations where higher values of $SD_{LL,D1+D2}$ are observed in Fig. 22; for example, between km 3.5 and 4.5 and between km 9 and 10.5. It is also interesting to note that most $\Delta SD_{LL,D1+D2}$ peaks are also centered on the track discontinuities identified above.

4.2 Dedicated Equipment

As part of a research project, the authors contributed to the development and testing of a prototype of a monitoring system mounted on a railway maintenance vehicle [71, 72]. To interpret the results obtained with part of this system [73], a methodology was developed for determining the railway track support conditions. This methodology is based on the modal analysis of the characteristic frequencies of a 2-DoF model composed of the railway infrastructure and an instrumented vehicle moving over it. The methodology is integrated in the group of vibration-based structural damage identification methods and is focused on observing the characteristic frequencies of the combined system, which can be correlated with changes in the physical properties of the infrastructure under analysis. By performing this assessment of the railway infrastructure across its length and over time, by comparing different rides over the same railway stretch, important information can be gathered about the track support conditions.

The sensors used to provide the data for this study (Fig. 25) consisted of two high-sensitivity ±4 g triaxial accelerometers, installed symmetrically in each vehicle's cabins. Four high-range ±500 g accelerometers, mounted on the wheel boxes, were used to measure the vehicle dynamic interactions with the track and to compare their output with the cabin accelerometers. The prototype also included two velocity

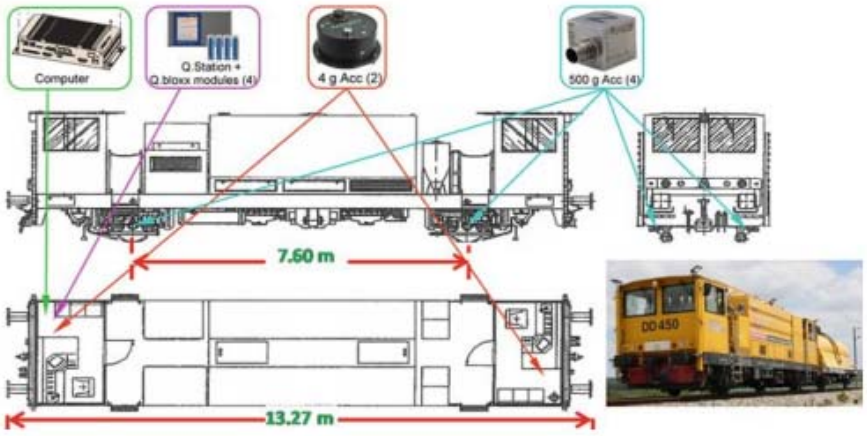

Fig. 25 Schematic view of the instrumentation locations in the railway vehicle [72]

sensors, installed on each shaft, and based on magnetic proximity sensors. The data generated by these velocity sensors, together with a GPS system, was used to obtain the position of the vehicle along the line. The data acquisition system collected data at a sampling frequency of 1000 Hz. This system comprised a data collector, some measuring modules and an industrial computer.

Preliminary validation of the developed methodology was performed by analyzing the passage of the instrumented vehicle over a transition zone between earthworks and a bridge [54, 73]. The comparison of on-board measurements with way-side measurements, allowed to conclude that the developed methodology is able to identify changes in functional and structural parameters of the railway line.

5 Final Remarks

This chapter presents some testing techniques, devices and monitoring systems that have been used for characterizing materials and for evaluating the structural behavior of the classic railway track. Some evaluation methods presented here are not yet commonly used, either due to the associated cost or to the need for qualified human resources. However, the improvement of knowledge and the technological advances in several areas will certainly allow their dissemination and widespread use.

References

1. Paixão, A., Varandas, J., Fortunato, E., Calçada, R.: Non-linear behaviour of geomaterials in railway tracks under different loading conditions. In: Advances in Transportation Geotechnics

3. Proceedings of the 3rd International Conference on Transportation Geotechnics, Guimarães, Portugal, 4–7 Sept 2016
2. Varandas, J., Paixão, A., Fortunato, E., Hölscher, P.: A numerical study on the stress changes in the ballast due to train passages. In: Advances in Transportation Geotechnics 3. Proceedings of the 3rd International Conference on Transportation Geotechnics, Guimarães, Portugal, 4–7 Sept 2016
3. Selig, E.T., Waters, J.M.: Track Geotechnology and Substructure Management. Thomas Telford, London (1994)
4. Indraratna, B., Salim, W., Rujikiatkamjorn, C.: Advanced Rail Geotechnology—Ballasted Track. Taylor & Francis (2011)
5. Varandas, J.N., Paixão, A., Fortunato, E., Zuada Coelho, B., Hölscher, P.: Long-term deformation of railway tracks considering train-track interaction and non-linear resilient behaviour of aggregates—a 3D FEM implementation. Comput. Geotech. **126**, 103712 (2020)
6. AREMA: Manual for Railway Engineering. American Railway Engineering and Maintenance-of-Way Association, Lanham, MD (2020)
7. CEN: European Standard EN 13450:2002, Aggregates for Railway Ballast. 93.100—Construction of Railways; 91.100.15—Mineral Materials and Products. CEN TC 154. Comité Européen de Normalisation, Brussels (2002)
8. Guo, Y., Markine, V., Zhang, X., Qiang, W., Jing, G.: Image analysis for morphology, rheology and degradation study of railway ballast: a review. Transp. Geotech. **18**, 173–211 (2019)
9. Blott, S.J., Pye, K.: Particle shape: a review and new methods of characterization and classification. Sedimentology **55**(1), 31–63 (2008)
10. Folk, R.L.: Student operator error in determination of roundness, sphericity, and grain size. J. Sediment. Petrol. **25**(4), 297–301 (1955)
11. Guo, Y., Zhao, C., Markine, V., Jing, G., Zhai, W.: Calibration for discrete element modelling of railway ballast: a review. Transp. Geotech. **23** (2020)
12. Quintanilla, I.D., Combe, G., Emeriault, F., Voivret, C., Ferellec, J.F.: X-ray CT analysis of the evolution of ballast grain morphology along a micro-Deval test: key role of the asperity scale. Granul. Matter **30**, 3–12 (2019)
13. Moaveni, M., Qian, Y., Boler, H., Mishra, D., Tutumluer, E.: Investigation of ballast degradation and fouling trends using image analysis. In: 2nd International Conference on Railway Technology: Research, Development and Maintenance—Railways 2014, Ajaccio, Corsica, France, 8–11 Apr 2014
14. Delgado, B.G., Viana da Fonseca, A., Fortunato, E., Goretti da Motta, L.M.: Particle morphology's influence on the rail ballast behaviour of a steel slag aggregate. Environ. Geotech. 1–10 (2019), published ahead of print
15. Al-Rousan, T.: Characterization of aggregate shape properties using a computer automated system. PhD thesis, Texas A&M University, Texas, 2004
16. Esmaeili, M., Nouri, R., Yousefian, K.: Experimental comparison of the lateral resistance of tracks with steel slag ballast and limestone ballast materials. Proc. Inst. Mech. Eng. Part F J. Rail Rapid Transit **231**(2), 175–184 (2017)
17. Delgado, B.G., Viana da Fonseca, A., Fortunato, E., Maia, P.: Mechanical behavior of inert steel slag ballast for heavy haul rail track: laboratory evaluation. Transp. Geotech. **20**, 100243 (2019)
18. Delgado, B.G., Viana da Fonseca, A., Fortunato, E., Paixão, A., Alves, R.: Geomechanical assessment of an inert steel slag aggregate as an alternative ballast material for heavy haul rail tracks. Constr. Build. Mater. **279**, 122438 (2021)
19. Suhr, B., Skipper, W.A., Lewis, R., Six, K.: Shape analysis of railway ballast stones: curvature-based calculation of particle angularity. Sci. Rep. **10**(1), 6045 (2020)
20. Jerónimo, P., Resende, R., Fortunato, E.: An assessment of contact and laser based scanning of rock particles for railway ballast. Transp. Geotech. **22**, 100302 (2020)
21. Paixão, A., Resende, R., Fortunato, E.: Photogrammetry for digital reconstruction of railway ballast particles—a cost-efficient method. Constr. Build. Mater. **191**, 963–976 (2018)

22. Zhao, L., Zhang, S., Huang, D., Wang, X., Zhang, Y.: 3D shape quantification and random packing simulation of rock aggregates using photogrammetry-based reconstruction and discrete element method. Constr. Build. Mater. **262**, 119986 (2020)
23. Paixão, A., Fortunato, E.: Abrasion evolution of steel furnace slag aggregate for railway ballast: 3D morphology analysis of scanned particles by close-range photogrammetry. Constr. Build. Mater. **267**, 121225 (2021)
24. Fortunato, E., Pinelo, A., Matos, F.M.: Characterization of the fouled ballast layer in the substructure of a 19th century railway track under renewal. J. Jpn. Geotech. Soc. Soils Found. **50**(1), 55–62 (2010)
25. Fortunato, E., Paixão, A., Fontul, S., Pires, J.: Some results on the properties and behavior of railway ballast. In: 10th International Conference on the Bearing Capacity of Roads, Railways and Airfields (BCRRA 2017), Athens, Greece, 28–30 June 2017
26. Werkmeister, S., Dawson, A., Wellner, F.: Permanent deformation behavior of granular materials and the shakedown concept. Transp. Res. Rec. **1757**, 75–81 (2001)
27. Stokoe II, K.H., John, S.H., Woods, R.D.: Some contributions of in situ geophysical measurements to solving geotechnical engineering problems. In: ICS-2 on Geotechnical and Geophysical Site Characterization, Porto (2004)
28. Fortunato, E., Bilé Serra, J., Marcelino, J.: Application of spectral analysis of surface waves (SASW) in the characterisation of railway platforms. In: International Conference on Advanced Characterization of Pavement and Soil Engineering Materials, Athens, 20–22 June 2007
29. Matthews, M.C., Hope, V.S., Clayton, C.R.I.: The use of surface waves in the determination of ground stiffness profiles. Proc. Inst. Civ. Eng. Geotech. Eng. **119**(2), 84–95 (1996)
30. Joh, S.-H.: Data Interpretation and Analysis for SASW Measurements. Chung-Ang University, Anseong, Korea (2002)
31. Burrow, M.P.N., Chan, A.H.C., Shein, A.: Deflectometer-based analysis of ballasted railway tracks. Proc. Inst. Civ. Eng. Geotech. Eng. **160**(3), 169–177 (2007)
32. Fontul, S., Fortunato, E., De Chiara, F.: Non-destructive tests for railway infrastructure stiffness evaluation. In: The Thirteenth International Conference on Civil, Structural and Environmental Engineering Computing, Crete, Greece, 6–9 Sept 2011
33. Fortunato, E., Fontul, S., Paixão, A., Cruz, N., Cruz, J., Asseiceiro, F.: Geotechnical aspects of the rehabilitation of a freight railway line in Africa. In: 3rd International Conference on Railway Technology: Research, Development and Maintenance—Railways 2016, Cagliari, Sardinia, Italy, 5–8 Apr 2016
34. Paixão, A., Alves Ribeiro, C., Pinto, N.M.P., Fortunato, E., Calçada, R.: On the use of under sleeper pads in transition zones at railway underpasses: experimental field testing. Struct. Infrastruct. Eng. **11**(2), 112–128 (2015)
35. UIC: Under Sleeper Pads—Summarising Report. Union Internationale des Chemins de Fer, Vienna (2009)
36. Paixão, A., Fortunato, E., Calçada, R.: Design and construction of backfills for railway track transition zones. Proc. IMechE Part F J. Rail Rapid Transit **229**(1), 58–70 (2015)
37. Varandas, J.N., Paixão, A., Fortunato, E.: A study on the dynamic train-track interaction over cut-fill transitions on buried culverts. Comput. Struct. **189**, 49–61 (2017)
38. De Man, A.P.: DYNATRACK: a survey of dynamic railway track properties and their quality. PhD thesis, Faculty of Civil Engineering, Delft University of Technology, Delft, 2002
39. Wu, T.X., Thompson, D.J.: Effects of local preload on the foundation stiffness and vertical vibration of railway track. J. Sound Vib. **219**(5), 881–904 (1999)
40. Alves, R.C., Paixão, A., Fortunato, E., Calçada, R.: Under sleeper pads in transition zones at railway underpasses: numerical modelling and experimental validation. Struct. Infrastruct. Eng. **11**(11), 1432–1449 (2015)
41. Quibel, A.: New in situ devices to evaluate bearing capacity and compaction of unbound granular materials. In: Gomes Correia, A. (ed.) Unbound Granular Materials—Laboratory Testing, In-Situ Testing and Modelling, pp. 141–151. A. A. Balkema, Rotterdam (1999)
42. Railways I.U.o.: IRS-70719:2020, Ed1: Railway Application—Track & Structure—"Earthworks and Track Bed Layers for Railway Lines"—Design and Construction Principles (2020)

43. Fortunato, E., Paixão, A., Fontul, S.: Improving the use of unbound granular materials in railway sub-ballast layer. In: Advances in Transportation Geotechnics II, Hokkaido University, Japan, 10–12 Sept 2012
44. Hosseingholian, M., Froumentin, M., Robinet, A.: Dynamic track modulus from measurement of track acceleration by Portancemetre. In: WCRR 2011—World Congress on Railway Research, Lille, France, 22–26 May 2011
45. Wang, P., Wang, L., Chen, R., Xu, J., Xu, J., Gao, M.: Overview and outlook on railway track stiffness measurement. J. Mod. Transp. **24**, 89–102 (2016)
46. Fontul, S., Antunes, M.L., Fortunato, E., Oliveira, M.: Practical application of GPR in transport infrastructure survey. In: International Conference on Advanced Characterization of Pavement and Soil Engineering Materials, Athens, Greece, 20–22 June 2007
47. Cruz, N., Fortunato, E., Asseiceiro, F., Cruz, J., Mateus, C.: Methodologies for geotechnical characterization in railways in operation. An experience. In: XVI European Conference on Soil Mechanics and Geotechnical Engineering, Edinburgh, United Kingdom, 13–17 Sept 2015
48. Fontul, S., Fortunato, E., De Chiara, F., Burrinha, R., Baldeiras, M.: Railways track characterization using ground penetrating radar. In: The 3rd International Conference on Transportation Geotechnics (ICTG 2016), Guimarães, 4–7 Sept 2016
49. De Chiara, F., Fontul, S., Fortunato, E.: GPR laboratory tests for railways materials dielectric properties assessment. Remote Sens. **6**(10), 9712–9728 (2014)
50. Fontul, S., de Chiara, F., Fortunato, E., Paixão, A.: Non destructive tests for evaluation of railway platforms—application of ground penetrating RADAR. In: 1st International Conference on Railway Technology: Research, Development and Maintenance (Railways 2012), Las Palmas, Gran Canaria, Spain, 18–20 Apr 2012
51. Fontul, S., Paixão, A., Solla, M., Pajewski, L.: Railway track condition assessment at network level by frequency domain analysis of GPR data. Remote Sens. **10**(4), 559 (2018)
52. Fontul, S., Fortunato, E., De Chiara, F.: Evaluation of ballast fouling using GPR. In: 15th International Conference on Ground Penetrating Radar—GPR 2014, Brussels, Belgium, 30 June–4 July 2014
53. Paixão, A., Fortunato, E., Calçada, R.: Transition zones to railway bridges: track measurements and numerical modelling. Eng. Struct. **80**, 435–443 (2014)
54. Paixão, A., Varandas, J., Fortunato, E., Calçada, R.: Numerical simulations to improve the use of under sleeper pads at transition zones to railway bridges. Eng. Struct. **164**, 169–182 (2018)
55. Paixão, A.: Transition zones in railway tracks. An experimental and numerical study on the structural behaviour. PhD thesis, University of Porto, Faculty of Engineering (FEUP), Porto (2014)
56. Aikawa, A.: Determination of dynamic ballast characteristics under transient impact loading. Electron. J. Struct. Eng. **13**(1), 17–34 (2013)
57. Jing, G., Siahkouhi, M., Edwards, J.R., Dersch, M.S., Hoult, N.A.: Smart railway sleepers—a review of recent developments, challenges, and future prospects. Constr. Build. Mater. **271**, 121533 (2021)
58. Rocchi, D., Tomasini, G., Schito, P., Somaschini, C., Testa, M., Cerullo, M., Arcoleo, G.: Ballast lifting: a challenge in the increase of the commercial speed of HS-trains. In: WCRR2016—11th World Congress on Railway Research, Milan, 29 May–2 June 2016
59. Mishra, D., Tutumluer, E., Boler, H., Hyslip, J.P., Sussmann, T.R.: Railroad track transitions with multidepth deflectometers and strain gauges. Transp. Res. Rec. J. Transp. Res. Board **2448**, 105–114 (2014)
60. CEN: European Standard EN 13848-5:2017 Railway Applications—Track—Track Geometry Quality—Part 5: Geometric Quality Levels—Plain Line, Switches and Crossings. 93.100—Construction of Railways. CEN/TC 256—Railway Applications. Comité Européen de Normalisation, Brussels (2017)
61. Esveld, C.: Modern Railway Track, Digital Edition 2016 edn. MRT-Productions, Zaltbommel, The Netherlands (2016)
62. CEN: European Standard EN 13848-2:2020 Railway Applications—Track—Track Geometry Quality—Part 2: Measuring Systems—Track Recording Vehicles. 93.100—Construction of

Railways. CEN/TC 256—Railway Applications. Comité Européen de Normalisation, Brussels (2020)
63. Weston, P., Roberts, C., Yeo, G., Stewart, E.: Perspectives on railway track geometry condition monitoring from in-service railway vehicles. Veh. Syst. Dyn. **53**(7), 1063–1091 (2015)
64. Paixão, A., Fortunato, E., Calçada, R.: Smartphone's sensing capabilities for on-board railway track monitoring: structural performance and geometrical degradation assessment. Adv. Civ. Eng. **2019** (2019)
65. Paixão, A., Fortunato, E., Calçada, R.: The effect of differential settlements on the dynamic response of the train-track system: a numerical study. Eng. Struct. **88**, 216–224 (2015)
66. Anthony, A.W.: Speech Recognition by Machine. Peter Peregrinus Ltd, London, UK (1988)
67. Berndt, D.J., Clifford, J.: Using dynamic time warping to find patterns in time series. In: KDD-94, Knowledge Discovery in Databases (AAAI-94), Seattle, WA, July–Aug 1994, pp. 359–370
68. Ubalde, L.: La auscultación y los trabajos de vía en la línea del AVE Madrid—Sevilla: análisis de la experiencia y deducción de nuevos criterios de mantenimiento. Ph.D. thesis, Universitat Politècnica de Catalunya, Barcelona, Spain, 2004
69. Kouroussis, G., Connolly, D.P., Alexandrou, G., Vogiatzis, K.: The effect of railway local irregularities on ground vibration. Transp. Res. Part D Transp. Environ. **39**, 17–30 (2015)
70. Paixão, A., Fortunato, E., Calçada, R.: A contribution for integrated analysis of railway track performance at transition zones and other discontinuities. Constr. Build. Mater. **111**, 699–709 (2016)
71. Santos, C., Morais, P., Paixão, A., Fortunato, E., Asseiceiro, F., Alvarenga, P., Gomes, L.: An integrated monitoring system for continuous evaluation of railway tracks for efficient asset management. In: 5th International Conference on Road and Rail Infrastructure (CETRA 2018), Zadar, Croatia, 16–19 Apr 2018
72. Morais, J., Santos, C., Morais, P., Paixão, A., Fortunato, E., Asseiceiro, F., Alvarenga, P., Gomes, L.: Continuous monitoring and evaluation of railway tracks: system description and assessment. In: The 3rd International Conference on Structural Integrity (ICSI2019), Funchal, 2–5 Sept 2019
73. Morais, J., Santos, C., Morais, P., Paixão, A., Fortunato, E., Asseiceiro, F., Alvarenga, P., Gomes, L.: Continuous monitoring and evaluation of railway tracks: proof of concept test. In: The 3rd International Conference on Structural Integrity (ICSI2019), Funchal, 2–5 Sept 2019